AD-A280 920

TATION PAGE

Form Approved
OBM No. 0704-0188

1. Agency Use Only *(Leave blank).*	2. Report Date.	3. Report Type and Dates Covered.
	1993	Final - Journal Article

4. Title and Subtitle.
Evidence for eddy formation in the eastern Arabian Sea during the northeast monsoon

5. Funding Numbers.
Program Element No. 0601153N
Project No. 03103
Task No. 030
Accession No. DN259010
Work Unit No. 573505504

6. Author(s).
Bruce, J. *, D. Johnson and J. Kindle

7. Performing Organization Name(s) and Address(es).
Naval Research Laboratory
Oceanography Division
Stennis Space Center, MS 39529-5004

8. Performing Organization Report Number.
JGU Vol. 99, No. C4, pp. 7651 -7664, April 15, 1994

9. Sponsoring/Monitoring Agency Name(s) and Address(es).
Office of Naval Research
800 N. Quincy St.
Arlington, VA 22217

10. Sponsoring/Monitoring Agency Report Number.
NRL/JA7332--93-0010

11. Supplementary Notes.
* Naval Oceanographic Office,
Stennis Space Center, MS

12a. Distribution/Availability Statement.
Approved for public release; distribution is unlimited.

12b. Distribution Code.

13. Abstract *(Maximum 200 words).*

The seasonal formation of a large (500-800 km diameter) anticyclonic eddy in the upper 300-400 m of the eastern Arabian Sea during the northeast monsoon period (December-April) is indicated from hydrographic and satellite altimetry sea level observations, as well as from numerical model experiments. The center of the eddy circulation is approximately 10 degrees N, 70 degrees E, just to the west of the north-south Laccadive Island chain. In this paper the eddy is called the Laccadive High (LH). In some ways it is a mirrorlike counterpart to the Great Whirl, which develops during the southwest monsoon off the Somali coast (western Arabian Sea). The LH occurs at the same latitude but on the opposite side of the basin during the reversed monsoon. It is different from the Great Whirl, however, in its formation process, its intensity, and its decay. The hydrographic data obtained from surveys all during a single season give sufficiently close station spacing to allow reasonable contouring of the geopotential surfaces and of the properties within and around the LH region with minimum time aliasing. The Geosat altimeter record extends over 4 years, during which the seasonal variability of the LH indicates a dynamic relief of approximately 15-20 cm, which is in good agreement with the hydrographic observations. The altimetry time series also suggests a westward translation of the OH by January with a subsequent dissipation in midbasin. The model used is a wind-forced three-layer primitive equation model which depicts a LH in agreement with the timing, position, and amplitude of both the hydrographic and altimetric measurements. The numberical simulation includes a passive tracer located in the western Bay of Bengal; the western advection of the tracer around the south coasts of Sri Lanka and India in December and January is consistent with the appearance of low-salinity water observed to extend into the Arabian Sea during this period. The modeling studies suggest that both local and remote forcing are important in the formation of the LH.

14. Subject Terms.	15. Number of Pages.
Air-sea interaction, ocean modeling, atmospheric modeling	14
	16. Price Code.

17. Security Classification of Report.	18. Security Classification of This Page.	19. Security Classification of Abstract.	20. Limitation of Abstract.
Unclassified	Unclassified	Unclassified	SAR

DISCLAIMER NOTICE

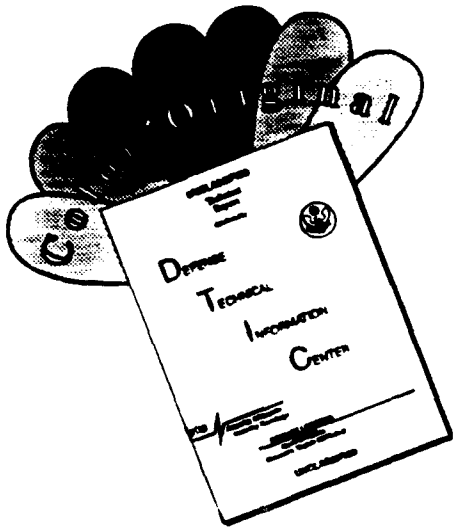

THIS DOCUMENT IS BEST QUALITY AVAILABLE. THE COPY FURNISHED TO DTIC CONTAINED A SIGNIFICANT NUMBER OF COLOR PAGES WHICH DO NOT REPRODUCE LEGIBLY ON BLACK AND WHITE MICROFICHE.

JOURNAL OF GEOPHYSICAL RESEARCH, VOL. 99, NO. C4, PAGES 7651–7664, APRIL 15, 1994

Evidence for eddy formation in the eastern Arabian Sea during the northeast monsoon

John G. Bruce
Naval Oceanographic Office, Stennis Space Center, Mississippi

Donald R. Johnson and John C. Kindle
Naval Research Laboratory, Stennis Space Center, Mississippi

Abstract. The seasonal formation of a large (500–800 km diameter) anticyclonic eddy in the upper 300–400 m of the eastern Arabian Sea during the northeast monsoon period (December–April) is indicated from hydrographic and satellite altimetry sea level observations, as well as from numerical model experiments. The center of the eddy circulation is approximately 10°N, 70°E, just to the west of the north-south Laccadive Island chain. In this paper the eddy is called the Laccadive High (LH). In some ways it is a mirrorlike counterpart to the Great Whirl, which develops during the southwest monsoon off the Somali coast (western Arabian Sea). The LH occurs at the same latitude but on the opposite side of the basin during the reversed monsoon. It is different from the Great Whirl, however, in its formation process, its intensity, and its decay. The hydrographic data obtained from surveys all during a single season give sufficiently close station spacing to allow reasonable contouring of the geopotential surfaces and of the properties within and around the LH region with minimum time aliasing. The Geosat altimeter record extends over 4 years, during which the seasonal variability of the LH indicates a dynamic relief of approximately 15–20 cm, which is in good agreement with the hydrographic observations. The altimetry time series also suggests a westward translation of the LH by January with a subsequent dissipation in midbasin. The model used is a wind-forced three-layer primitive equation model which depicts a LH in agreement with the timing, position, and amplitude of both the hydrographic and altimetric measurements. The numerical simulation includes a passive tracer located in the western Bay of Bengal; the western advection of the tracer around the south coasts of Sri Lanka and India in December and January is consistent with the appearance of low-salinity water observed to extend into the Arabian Sea during this period. The modeling studies suggest that both local and remote forcing are important in formation of the LH.

Introduction

In response to an annual cycle of differential heating and cooling between the Indian Ocean and the Eurasian Continent, the equatorial and northern Indian Ocean experiences extraordinary north/south excursions of the Intertropical Convergence Zone (ITCZ). Heavy rainfall as well as reversals of wind stress, concomitant with reversals of ocean surface currents, accompany the semiannual sweeps of the ITCZ across this area. The effects of these reversals are especially dramatic in the Arabian Sea, where the SW monsoon (boreal summer) attains high wind speeds in a concentrated jet stream (Findlater Jet) flowing along the East African Highlands [*Findlater*, 1977] and out across the Arabian Sea. Many previous observational programs have concentrated on this season and on the Somali Current and Oman coastal regions, since the effects there are particularly pronounced. Less attention has been paid to the NE monsoonal season and to the eastern Arabian Sea. Regional geography and schematics of seasonal currents are presented in Figure 1.

This paper focuses on a newly recognized large anticyclonic eddy that forms in the Laccadive Island regions (Figure 1) during the NE monsoon. This eddy, which we will call the "Laccadive High" (LH) is, in many ways, a mirrorlike counterpart of the Great Whirl [*Bruce*, 1981] found off the northern tip of Somalia. It occurs at the same latitude, but on the opposite side of the Arabian Sea basin, and in the opposite monsoon season. As we shall see, however, it is significantly different in its formation and decay processes and in its intensity. We will discuss the climatological setting and in situ observations of the LH, satellite altimetric observations of its temporal characteristics, and modeling results that simulate some of its features.

Climatological Wind and Current Patterns During the NE Monsoon

In Plate 1, climatological wind stress and curl of the wind stress [*Hellerman and Rosenstein*, 1983] (hereinafter referred to as HR) are given over the Arabian Sea for January (NE monsoon) and July (SW monsoon). During both seasons

Paper number 94JC00035.

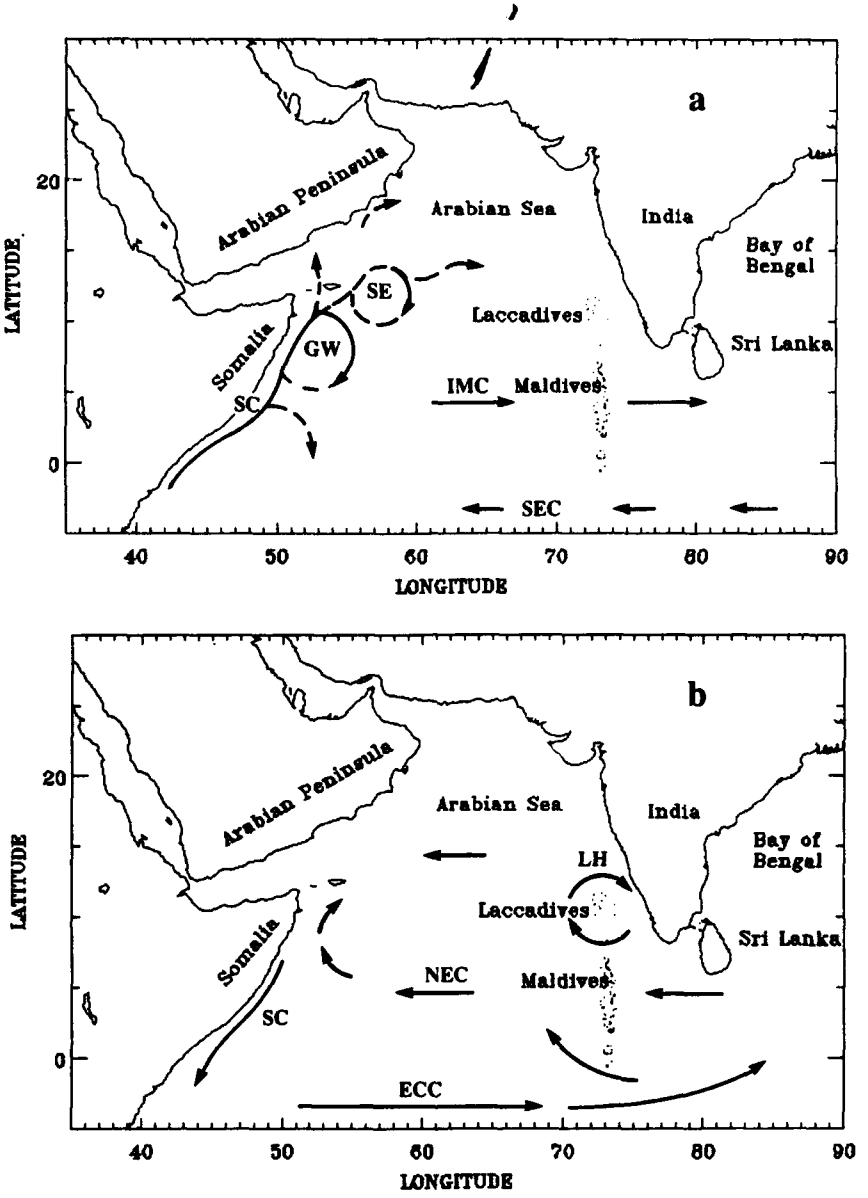

Figure 1. Indian Ocean currents and eddies [after *Molinari et al.*, 1990]. (a) Boreal summer (SW monsoon) and (b) boreal winter (NE monsoon). Abbreviations are SC, Somali Current; GW, Great Whirl; SE, Socotra Eddy; IMC, Indian Monsoon Current; SEC, South Equatorial Current; NEC, North Equatorial Current; ECC, Equatorial Countercurrent; LH, Laccadive High.

the wind stress maximum amplitude is found off the coast of Somalia. However, the direction of stress reverses, and the curl changes sign from NE to SW monsoons. Of particular interest is the strength of the negative wind stress curl off the coast of Somalia in the Great Whirl area and off the southwestern tip of India in the LH area.

The Indian subcontinent significantly alters the direction and magnitude of the surface wind patterns over the Arabian Sea and the Bay of Bengal. During the SW monsoon (Plate 1a) the winds in the eastern Arabian Sea shift to westerlies south of 10°N and return to southwesterlies in the Bay of Bengal. The region of negative wind stress curl extends over most of the Arabian Sea and has been shown to be an important factor in the physical and biological ocean response during this season [e.g., *Luther and O'Brien*, 1985; *Bauer et al.*, 1991; D. K. Young and J. C. Kindle, Importance of physical and biological processes to silicon imitation of diatom production in the Arabian Sea, submitted to *Journal of Geophysical Research*, 1994]. During the NE monsoon (Plate 1b) the surface flow exhibits two distinct jets in the Arabian Sea and the Bay of Bengal, respectively. While the former is the most intense, the jet that crosses into the southern Arabian Sea near Sri Lanka is sufficiently strong to generate an intense patch of negative wind stress curl off the southwest coast of India. This "funneling of the northeast trades between India and Sri Lanka" was also noted by *Hastenrath and Lamb* [1979, Charts 14 and 15]. It is interesting that, although the strongest winds during the NE monsoon are over the western Arabian Sea, the region of maximum negative wind stress curl is in the southeastern Arabian Sea. This is caused by (1) the close proximity of the westernmost jet to the Somali coast, thereby preventing the

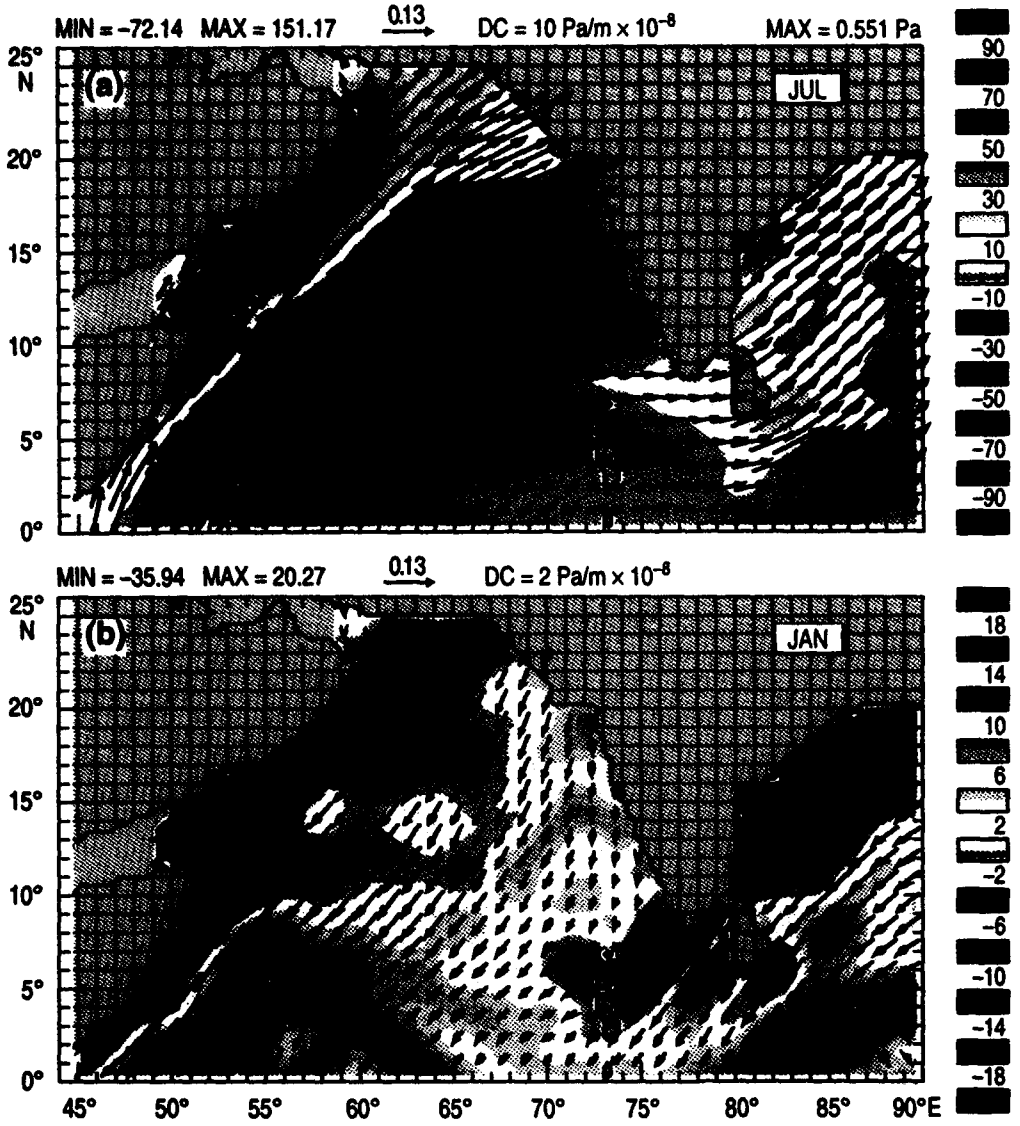

Plate 1. Climatological wind stress vectors superimposed with contours of wind stress curl for (a) July and (b) January from the *Hellerman and Rosenstein* [1983] climatology. Arrows indicate wind direction and speed. Note the change in contour interval from SW monsoon to NE monsoon. The maximum negative wind stress curl during the NE monsoon is approximately half of that during the SW monsoon. The contour intervals are (a) 10×10^{-8} Pa/m and (b) 2×10^{-8} Pa/m.

appearance of strong negative curl over the ocean, and (2) the funneling of the jet near Sri Lanka, as discussed above, together with the patch of very weak winds off the southwest Indian coast, which produces an asymmetry to the jet and enhances the negative curl.

Although the NE monsoon is the less energetic of the two monsoons in the Arabian Sea, the near-surface ocean circulation is still dominated by the wind system during this period. The wind direction tends to be relatively steady, and the wind speed is moderate, albeit somewhat weaker than during the SW monsoon. Table 1 (for the region 7°N–10°N, 70°E–75°E) shows that the dominant wind direction during the NE monsoon tends to shift gradually from northeast (December) to northwest (April). Wind speeds during this time are about 3.5 m s^{-1}, with a relatively high wind steadiness of 80–90% in the eastern Arabian Sea [*Hastenrath and Lamb*, 1979].

Climatological surface current charts from 120 years of ship drift observations [*Cutler and Swallow*, 1984] give clear evidence of a relatively strong westward flow (30–70 cm s^{-1}) between 3°N and 7°N across the Maldive Island chain (~72°E) during the NE monsoon. To the west of the Maldive Islands, part of the flow tends to turn northwest and then north near 10°N in an anticyclonic pattern. The origin of the current appears to be from water in the southwestern Bay of Bengal, which is relatively fresh (32–34‰). Surface salinity maps (Figure 2) clearly demonstrate westward penetration of low-salinity water from the Bay of Bengal into the Arabian Sea [*Wyrtki*, 1971].

In Situ Observations

The International Indian Ocean Expedition (IIOE) hydrographic surveys during both the 1963 SW monsoon and the

Table 1. Northeast Monsoon Winds

Month	Wind Direction, %			Winds From NE to NW Quadrant		Percent Calm	Average Speed NE to NW Quardrant, m/s
	NW	N	NE	Percent	Number Observation		
Nov.	9	8	14*	31	7858	7	3.0
Dec.	8	27	35*	70	7564	9	3.6
Jan.	5	34	38*	77	8227	8	3.6
Feb.	12	44*	25	81	4759	9	3.6
March	24	35*	15	74	8681	13	3.0
April	35*	18	6	59	8734	11	3.6
May	33*	7	2	42	7622	4	4.0

Winds from area 7 (7°N–10°N, 70°E–75°E). Data are from *Naval Air Weather Service* [1976].
*Dominant wind direction.

1965 NE monsoon in the Arabian Sea indicated the approximate horizontal scales and geopotentials of mesoscale eddies occurring in response to wind stress. This paper reexamines these early results from the NE monsoon, in particular because there is evidence that the relatively large anticyclonic eddy occurring in the SE Arabian Sea (LH), which was determined from these hydrographic observations is generated during each NE monsoon.

A comparison between the NE and SW monsoon sea surface geopotentials (relative to 1000 dbar) along zonal hydrographic sections at 10°N (Figure 3) from the IIOE surveys shows that the largest high ($>1.8 \times 10\ m^2\ s^{-2}$) during either season occurred between 66°E and 73°E during the NE monsoon [*Bruce*, 1968]. The dimensions of this high are comparable in magnitude to those found during the SW monsoon in the western portion of the section (52°E–63°E), which include the Great Whirl (farthest west in Figure 3) and what appears to be another relatively large anticyclonic structure (~60°E, possibly associated with the Socotra Eddy [*Bruce and Beatty*, 1985]). During the SW monsoon the eastern portion of the section shows a decrease in geopotential ($<1.5 \times 10\ m^2\ s^{-2}$), considerably below the mean of the sections.

The meridional volume transport across 10°N associated with the circulation around the anticyclonic eddies during the monsoons (Figure 4) shows a transport around the LH of 15–19 Sv ($1\ Sv = 10^6\ m^3\ s^{-1}$). This is roughly 50% of that observed in the Great Whirl during the SW monsoon (30–40 Sv) [*Bruce and Beatty*, 1985]. In general, the largest meridional transports are in the eastern portion of the 10°N section during the NE monsoon and in the western portion during the SW monsoon.

During the IIOE 1965 NE monsoon survey, both *Atlantis II* and *Meteor* obtained sufficient observations in the eastern Arabian Sea such that the geopotential of the sea surface could be mapped over the LH (Figure 5). The eddy center is found near 10°N/70°E, just west of the Laccadive/Maldive Island Chain. The geopotential at the center is greater than

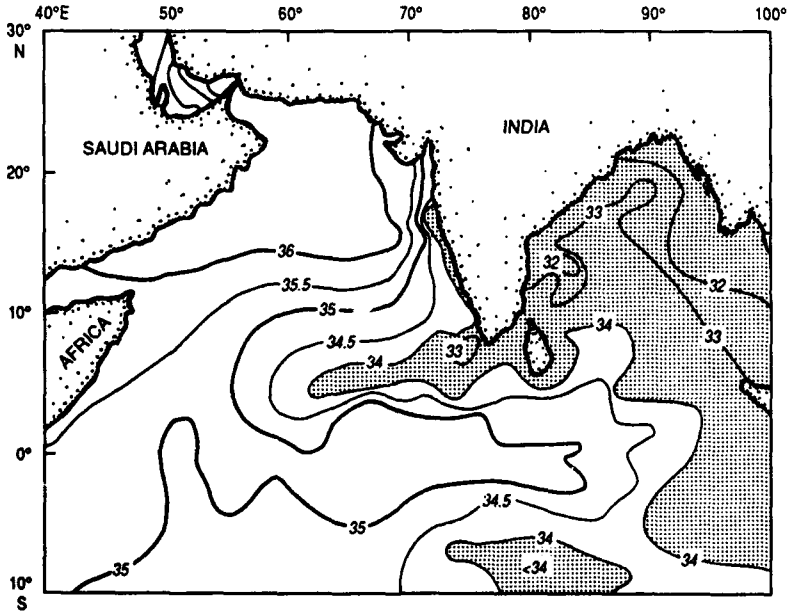

Figure 2. Surface salinity (per mil) during January and February showing penetration of fresh plume from Bay of Bengal into southern Arabian Sea [after *Wyrtki*, 1971].

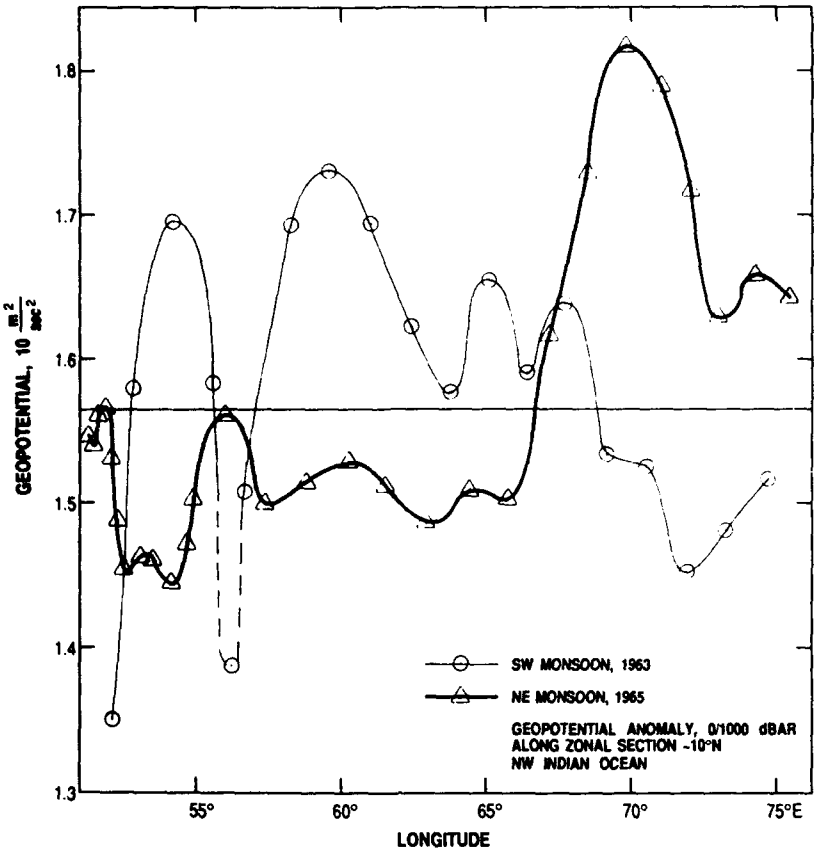

Figure 3. Comparisons of geopotential anomaly, 10 m^2 s^{-2}, from hydrographic zonal sections obtained during both the NE and SW monsoons along approximately 10°N in the Arabian Sea. Dashed portion of line gives estimated value obtained from bathythermograph data [after *Bruce*, 1968].

1.8 × 10 m^2 s^{-2}. This represents a dynamic topographic relief of about 15–20 cm above its surroundings (Figure 5).

Symmetry of flow around the central region of the eddy is indicated by the vertical distribution of the northgoing and southgoing geostrophic currents (Figure 6) across the section, as well as by the distribution of salinity (Figure 7). The speeds of the geostrophically calculated surface currents (30–40 cm s^{-1}) correspond to the climatological speeds of the westward flow through the Laccadive/Maldive Island Chain during this monsoon period. The circulation is clearly surface intensified with the strongest flow trapped in the upper 100–150 m, decaying to 10 cm s^{-1} at the 250–300 m level.

The sources of the relatively fresh surface salinity (<33.8‰) at the eddy center (Figure 7) are most likely from the Bay of Bengal (Figure 2), probably augmented by coastal runoff along the southwest coast of India. This low-salinity core is contained in a relatively shallow layer, from the surface to ~100–150 m. A further look at the low-salinity source will be presented later in this paper in a model tracer experiment.

Satellite Altimetry

As shown by *Perigaud and Minster* [1988], the seasonally occurring mesoscale features in the Indian Ocean tend to be well suited for satellite altimetric studies (see also *Perigaud and Delecluse* [1992] and *Arnault and Perigaud* [1992]). They were able to favorably compare Seasat altimetry with dynamic topography estimated from repeated expendable bathythermograph (XBT) sections across eddies associated with the Somali Current in the western Arabian Sea during August 1978 [*Bruce*, 1981]. For regions that lack a suitable marine geoid, altimetric observations are commonly used in mapping the variability of sea surface dynamic topography, that is, anomalous departures from a mean reference surface that includes the marine geoid and the mean dynamic topography. Since annual variations about the mean in the Arabian Sea are large, the eddies are well represented as anomalies.

With its launch in early 1985, the U.S. Navy's Geosat altimeter has provided a remarkable record of sea surface dynamic topography, covering more than 4 $\frac{2}{3}$ years until its demise in January 1990. For the first 18 months of the mission (April 1985 to October 1986), Geosat's raw observations along nonrepeat orbits were classified for naval purposes. However, the temporal variations of sea surface topography, as obtained from crossover point differences, were open to the scientific community. Beginning in the fall of 1986, Geosat entered into its unclassified Exact Repeat Mission (ERM).

Crossover points are the intersections along ground tracks of ascending and descending satellite passes. After proper corrections for environmental effects, tides and long-wavelength orbital errors, the differences in sea level be-

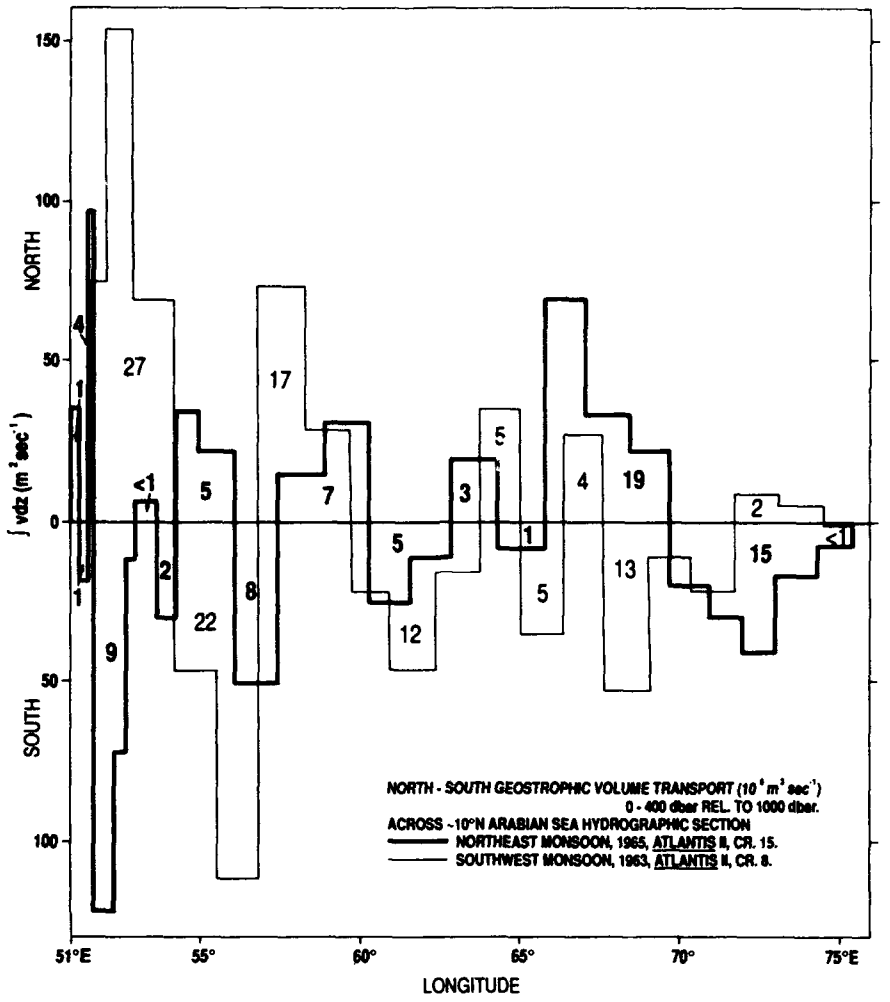

Figure 4. Meridional geostrophic volume transport ($\times 10^6$ m^3 s^{-1}) across ~10°N hydrographic sections during monsoons. Sections extend from (left) Somalia to (right) India.

tween passes at crossover points represent temporal variations in dynamic topography (commonly defined as sea surface height (SSH) anomalies). In this study we use Geosat altimetry data, which cover the entire mission from the Naval Oceanographic Office and from the National Oceanic and Atmospheric Administration (NOAA).

NOAA very kindly supplied a time series of SSH anomalies in the area around 10°N/70°E, which were constructed for the period of the classified mission from crossover point differences, and for the ERM from collinear differences, averaged over 1° latitude by 2° longitude bins. These anomalies were referenced to a 12-month mean from August 1987 to July 1988. The results shown in Figure 8 clearly indicate the seasonal signal of the LH as well as the low occurring during the SW monsoon. The range of sea level anomaly, which is of the order of 10–20 cm above the mean, is in reasonably good agreement with the range in geopotential anomaly found during the IIOE hydrographic survey (Figure 5). The creation of the eddy appears to take place much more rapidly than its decay, as indicated by the temporal asymmetry of the curve in Figure 8.

To obtain a spatial representation of the development and decay of the LH, Geosat crossover point differences were examined during the nonrepeat orbit classified mission for the boreal winter of 1985/1986. The reason for using this data set was for its excellent spatial pattern of observation. Crossover point differences were binned into diamond-shaped grids in a manner discussed by *Johnson et al.* [1992], and time series of SSH anomalies were formed for each grid point in the manner of *Fu and Chelton* [1985]. The grids were 3° latitude by 3° longitude in size and nested with grid points at 1° latitude and longitude intervals.

Snapshots of the resulting SSH anomaly topography at 30-day intervals during the LH buildup and at 9-day intervals during the final decay period are presented in Figure 9. The buildup took place rapidly, with the first indication of formation at year day 328 (November 24, 1985), reaching maximum development about 30 days later. In another 30 days there is clear indication of movement toward the west (offshore), and by February 22, 1986, the eddy can be located over 800 km west of its initial position. In its final stages the eddy decays in amplitude, becomes distorted, and breaks up. At maximum development the altimetric anomaly shows about 10–12 cm of relief. Because of the manner in which the crossover point difference time series are formed from data over a 3° × 3° area, it can be expected that the amplitude will be reduced by this method.

In Figure 10, time series of the SSH anomalies are

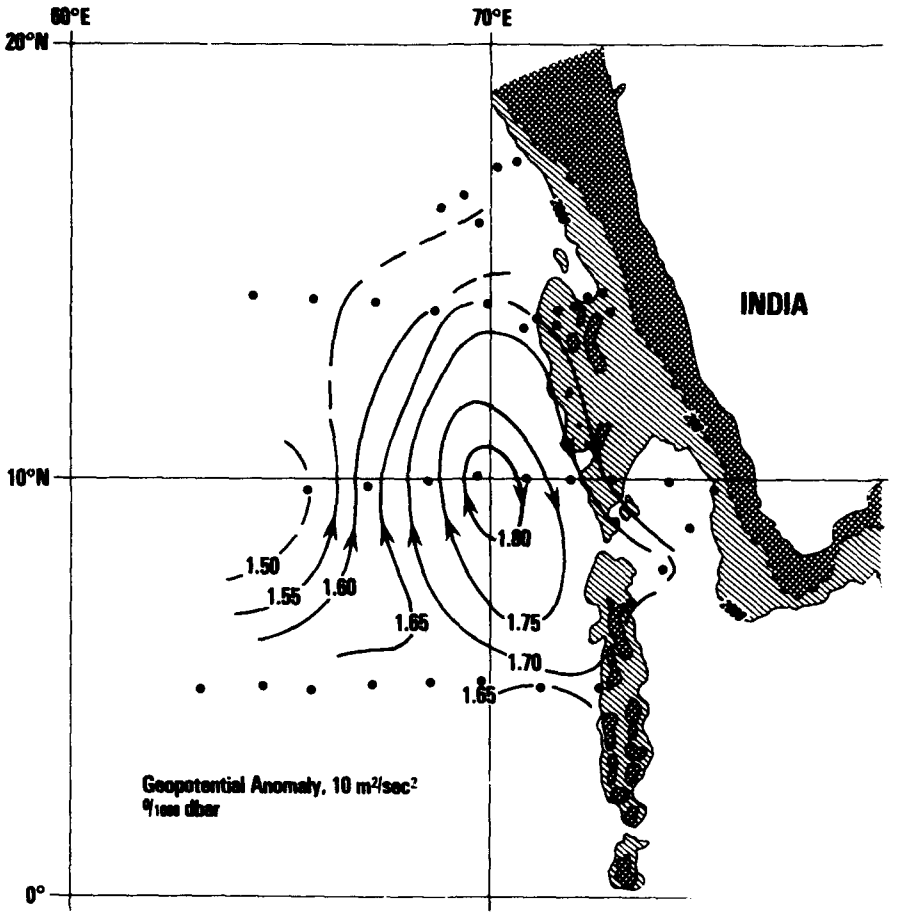

Figure 5. Sea surface geopotential anomaly, 10 m^2 s^{-2} 0/1000 dbar, contoured using *Atlantis II*, cruise 15, and *Meteor* stations, February through April 1965, International Indian Ocean Expedition.

presented at longitudinal positions along a latitude line of 9.75°N. Movement of the eddy can easily be traced as a function of time along this line. Movement to the west occurs with a propagation speed of about 16–18 cm s^{-1}, until the eddy reaches about 63°E to 64°E. By that time the eddy amplitude has been reduced, and it appears to begin breaking up. A second appearance of a SSH high off the tip of India occurs at year day 445 (March 21, 1986) but dies quickly in place (Figures 9 and 10).

Model Comparison

Results from a wind-forced, three-layer, reduced-gravity, primitive equation model of the entire Indian Ocean were examined for evidence of the appearance of the LH. The model is derived from the two-layer formulation of *Hurlburt and Thompson* [1980] with significant enhancements added by *Wallcraft* [1991]. The model domain, which includes the entire Indian Ocean north of 30°S and west of 110°E, gridded to a resolution of 0.4°, is identical to the hydrodynamic, one-layer, reduced-gravity, Indian Ocean model discussed by *Kindle and Thompson* [1989] and *Kindle* [1991]. The present version includes thermodynamic effects and permits horizontal density gradients within each layer. The density is modified by entrainment, detrainment, advection, diffusion, surface heat flux, and relaxation to a mean density climatology based on *Levitus* [1982]. For the experiments in this report, no surface heat fluxes were applied. Model parameters are provided in Table 2.

The wind stress for the numerical simulation is the *Hellerman and Rosenstein* [1983] wind stress climatology with linear interpolation between mean monthly values. The model experiment is performed in three steps: (1) a hydrodynamic version of the model is started from rest and run for 10 years forced by the HR climatology; (2) subsequently, the model density climatology is formed by averaging the *Levitus* [1982] values over the mean layer thickness at each point, and (3) the model is initialized from the hydrodynamic experiment and resulting density climatology and run for 15 years, forced by the HR stresses. Statistical equilibrium is reached by year 10.

Snapshots during the NE monsoon of the model sea surface superimposed with upper layer currents are shown in Plate 2 for a portion of the model domain. The first panel (Plate 2a) depicts the model circulation in mid-October. At this time there is little indication of the LH. The most prominent features are the remnants of the Great Whirl and Socotra Eddy in the northwest Arabian Sea. In association with the establishment of the NE monsoon, however, the North Equatorial Current (NEC) forms between the equator and 5°N (Plate 2b) in agreement with the descriptions of the Indian Ocean surface currents as provided by *Cutler and Swallow* [1984] and *Molinari et al.* [1990]. The westward

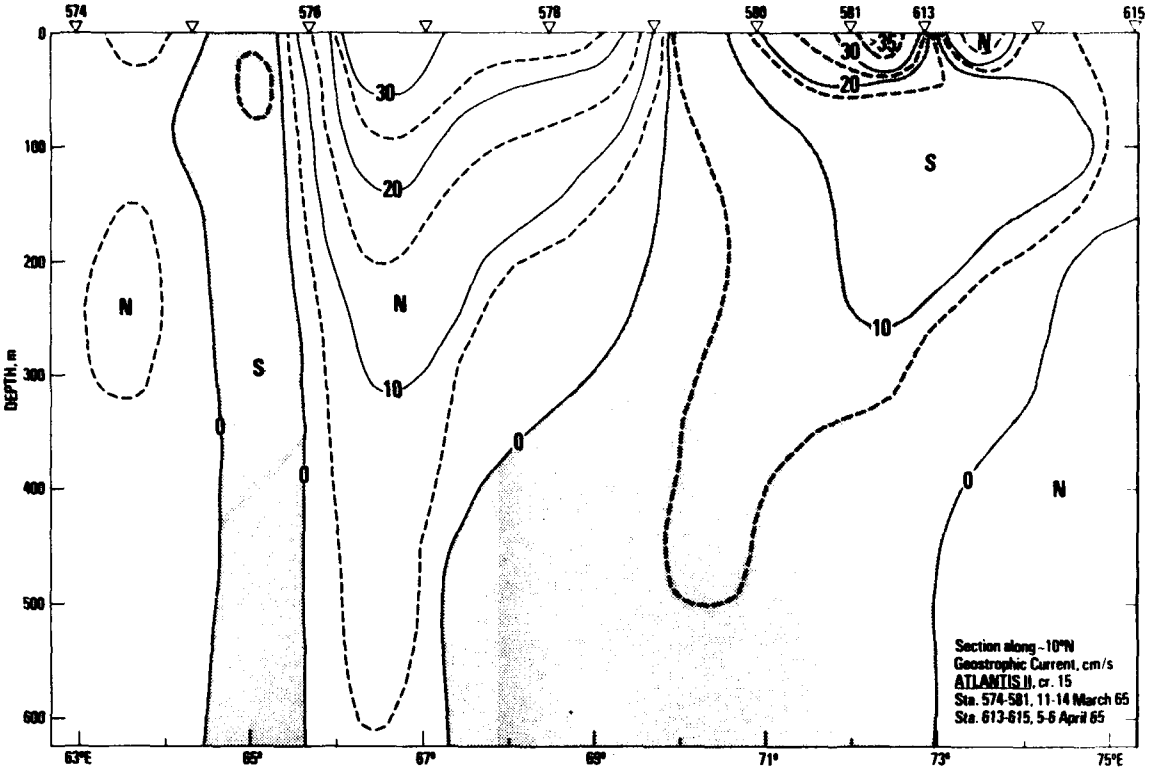

Figure 6. Geostrophic baroclinic current cm s^{-1}, across 10°N zonal section through eddy (center near station 579).

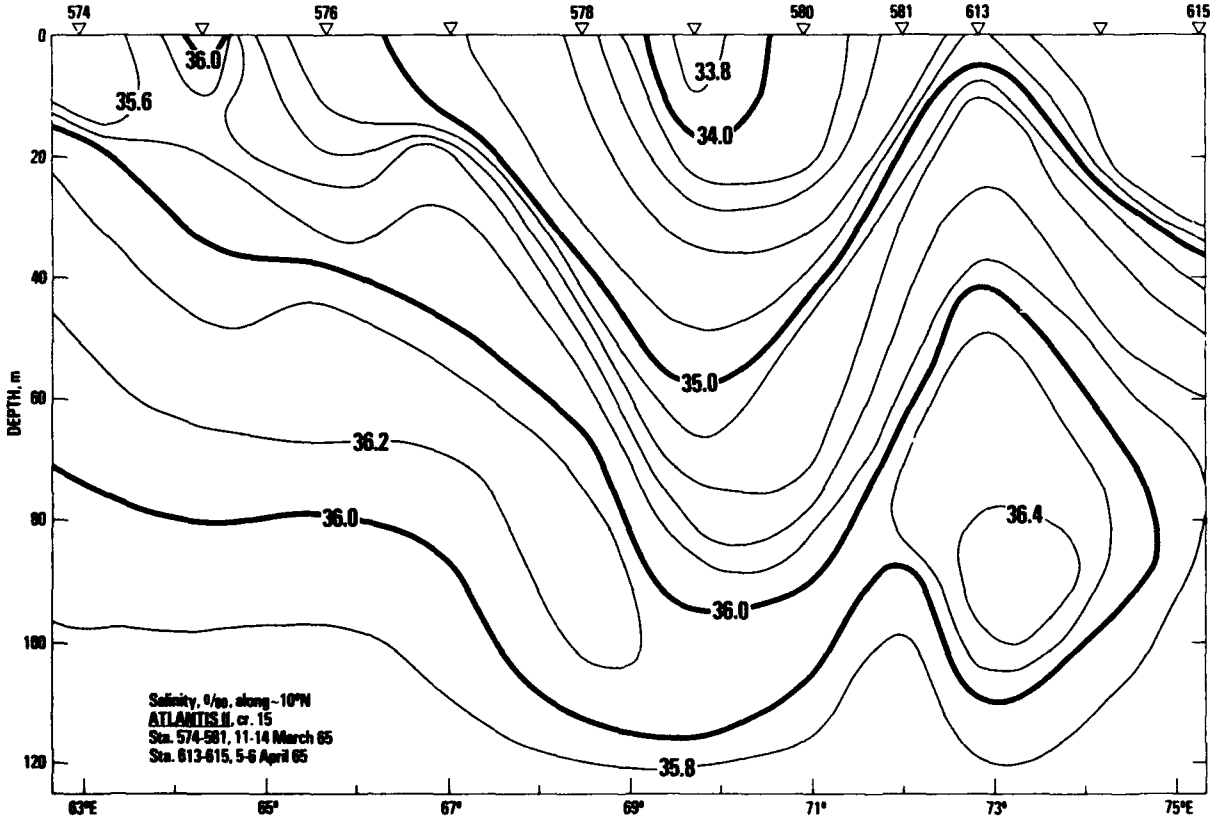

Figure 7. Distribution of salinity (per mil) on 10°N zonal section through eddy. Note relative symmetry to east and west of station 579 near eddy center.

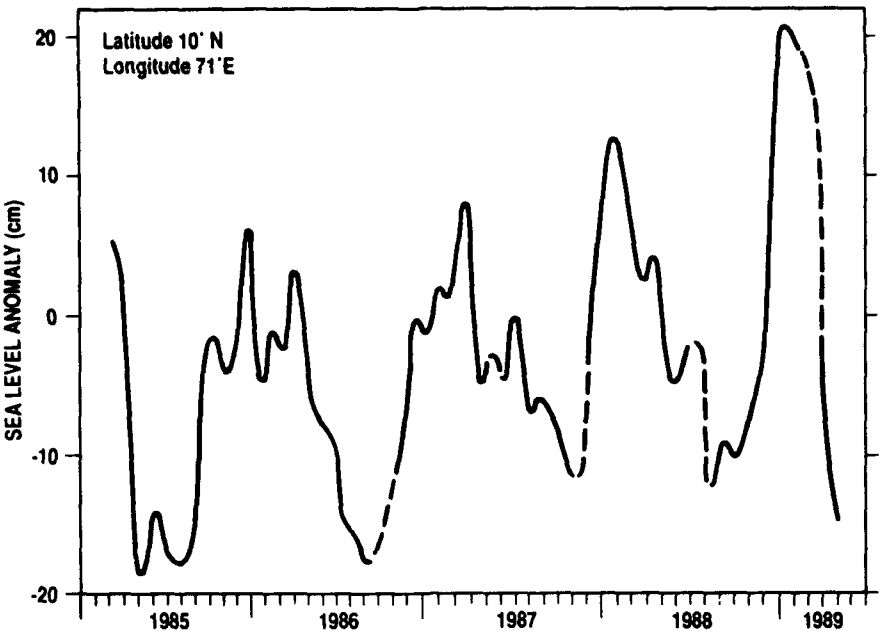

Figure 8. Sea surface height anomaly from Geosat altimetry relative to 1-year mean from August 1987 and 1988 for the time period March 1985 through April 1989 in the region centered at 10°N 71°E (area 1° latitude, 2° longitude).

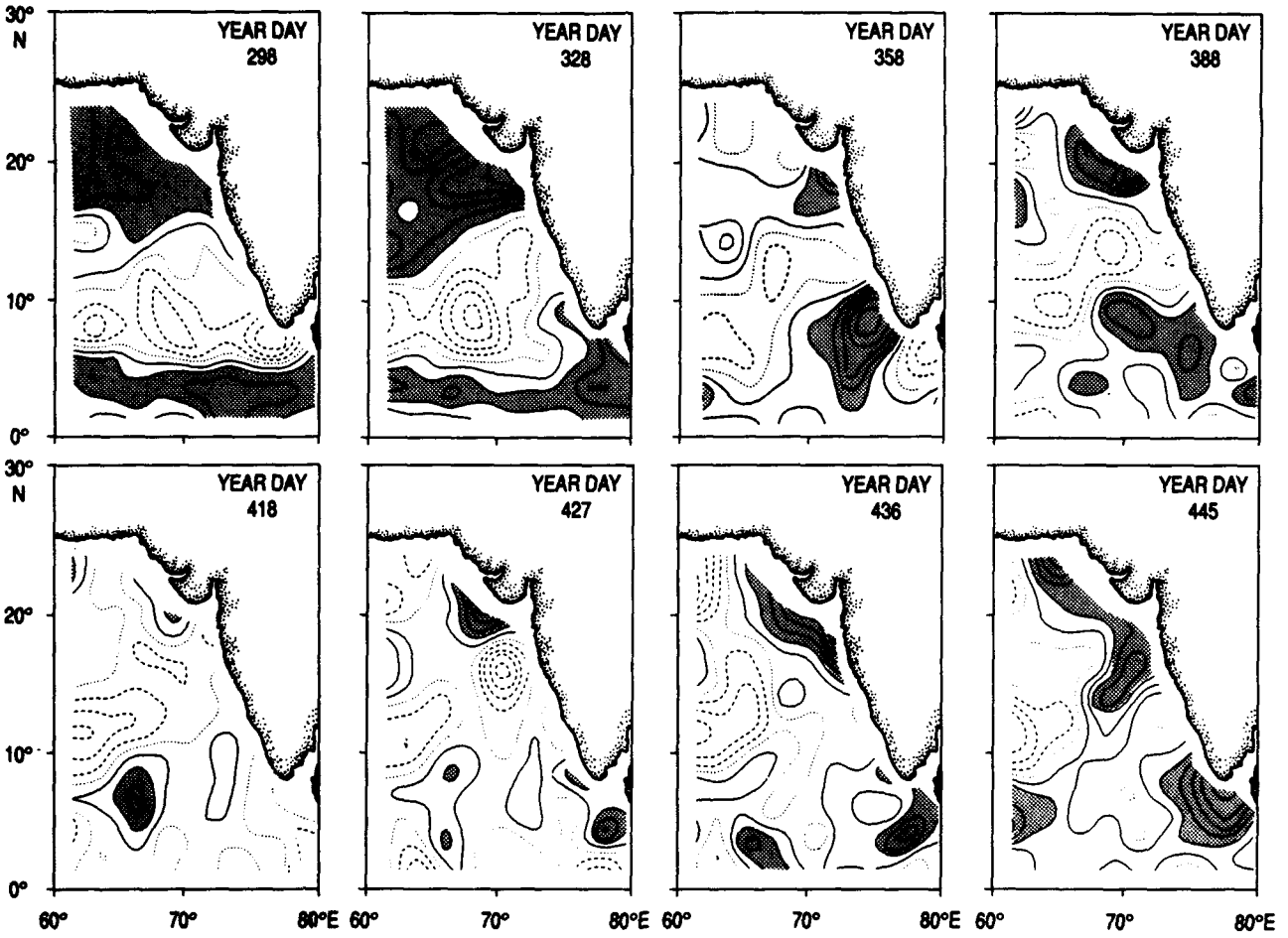

Figure 9. Sea surface height anomaly from Geosat altimetry relative to a 1-year mean. Year day is referred to January 1, 1985. Contours are in 2.5-cm intervals, positive is solid, negative is dashed, greater than 2.5 cm is shaded. Upper panel at 30-day intervals, lower panel at 9-day intervals. Full development of the LH is reached by year day 358.

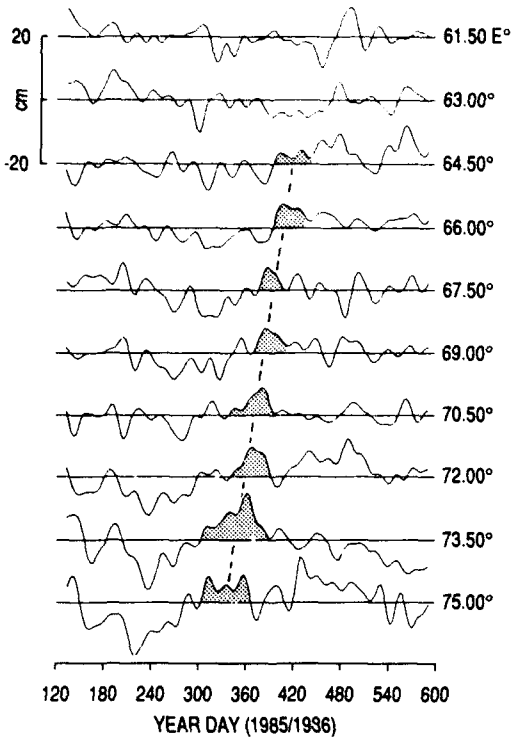

Figure 10. Time series of SSH anomalies from Geosat at longitudes along the 9.75° latitude line. The shaded highs are spatial/temporal displacements of LH as it migrates toward the west at a speed of 16–18 cm s^{-1}.

flowing NEC feeds the Somali Current in the west and the northward flow along the west Indian coast from December to February. Coincident with the intensification of the NE monsoon in December is the appearance of the LH off the southwest coast of India (Plate 2b).

The formation of the model LH is consistent in timing, position, and amplitude with the in situ observations and satellite altimetry discussed above. The generation of the model LH off the coast of India and its subsequent westward propagation are phenomena that occur every year, regardless of whether the model is forced by climatological winds or by stresses from operational centers for particular years. The Laccadive High appears to be linked to the strong negative wind stress curl associated with the NE monsoon in December and January (Plate 1b).

If the LH is generated in place off the southwest coast of India, then an intriguing issue arises as to the origin of the low-salinity water observed within the eddy. This point was investigated by including a passive tracer in the numerical simulation described above. The source of the tracer is in the upper layer of the Bay of Bengal within a rectangle defined by 80°W to 83°W and 10°N to 15°N, that is, within the low-salinity region shown in Figure 2. The advection and diffusion of the tracer are governed by identical formulations for the model density. Snapshots of the model tracer coincident with the circulation plots (Plate 2) are shown in Plate 3. Throughout most of the year, the model circulation restricts the extent of the tracer to the Bay of Bengal. However, in December the establishment of the NE monsoon generates southward flow along the southeast coast of India and Sri Lanka and a convergence with the NEC (Plate 2b). Hence in December and January the NEC advects western Bay of Bengal Surface Water into the Arabian Sea (Plates 3a and 3b). The bifurcation of the NEC (Plates 2b and 2c) just east of the Maldives allows the low-salinity water to be entrained into the LH (Plates 3c and 3d) during its formation period. The westward advection of the tracer by the NEC and the propagation of the LH offshore yield a tongue of Bay of Bengal Water in February that is quite similar to that shown by *Wyrtki* [1971] (Figure 2). In March and April (not shown) the model NEC slows and turns southward to feed the Equatorial Jet (Figure 1) generated during the monsoon transition [*Wyrtki*, 1973; *O'Brien and Hurlburt*, 1974]. This strong eastward flow, together with the Indian Monsoon Current (Figure 1) during the SW monsoon, return the low-salinity surface water back to the Bay of Bengal. Hence the distribution of the model tracer illustrates the mechanisms which would allow the LH to be generated off the southwest coast of India while containing a core of low-salinity water, apparently from the Bay of Bengal.

Table 3. Characteristics of the Laccadive High

Parameter	Value
Diameter	500–800 km
Depth	300–400 m
Swirl velocity	30–35 cm s^{-1} at the surface
Swirl transport	15–19 Sv
Dynamic relief	15–20 cm
Westward migration rate	16–18 cm s^{-1}
History	seasonal recurrence during NE monsoon (December to March)

Table 2. Model Parameters

Parameter	Definition	Value
A_m	eddy viscosity (momentum)	1000 m^2 s^{-1}
A_d	eddy viscosity (density)	2500 m^2 s^{-1}
g	acceleration of gravity	9.8 m s^{-2}
H_1, σ_1	undisturbed upper layer depth, density	100 m, 23.41
H_2, σ_2	undisturbed second layer depth, density	200 m, 25.87
H_3, σ_3	undisturbed third layer depth, density	250 m, 26.79
σ_4	lowest layer density	27.71
Δx, Δy	horizontal grid spacing	0.4°
Δt	time step	36 min

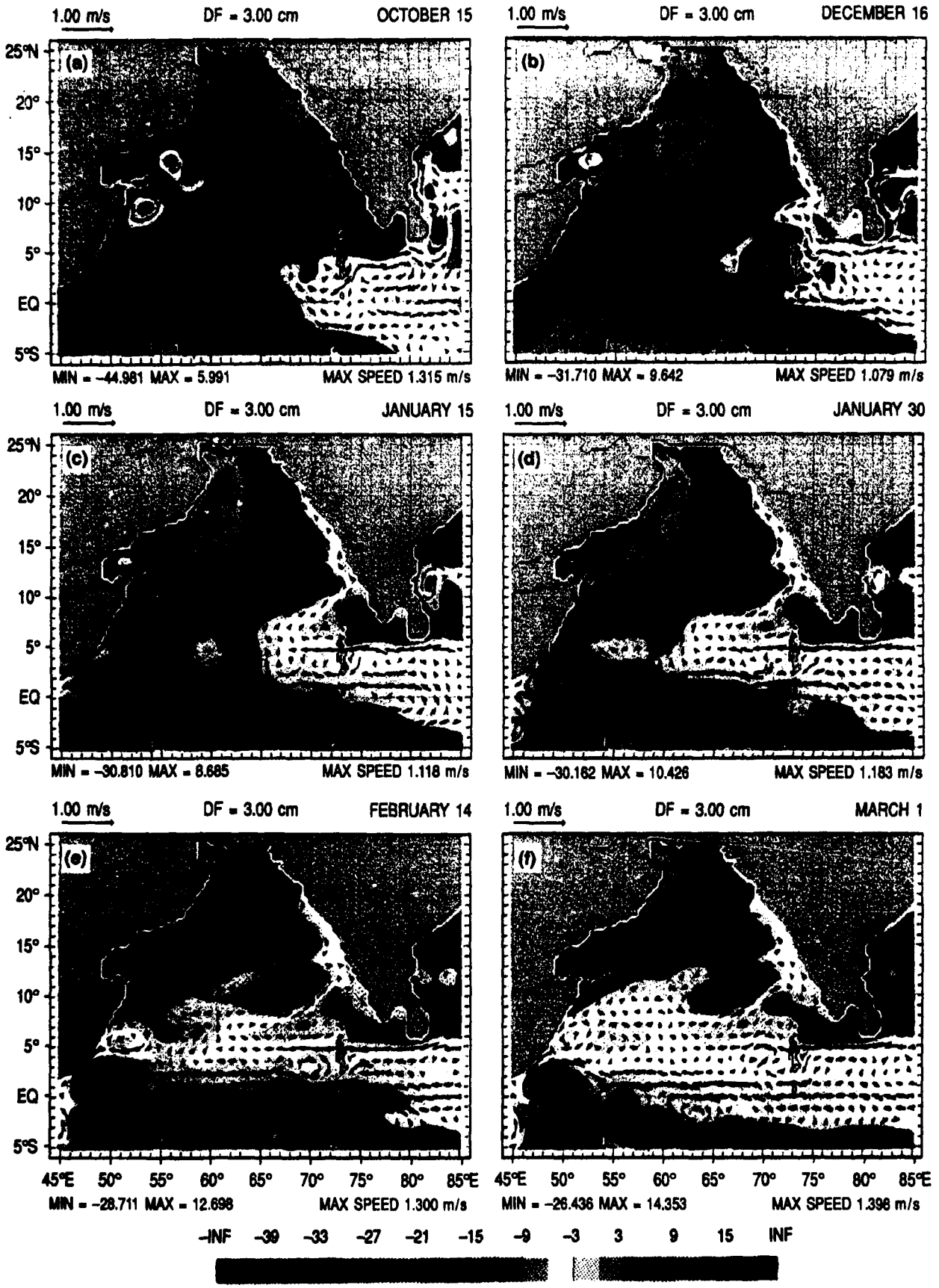

Plate 2. Snapshots of the model sea surface superimposed with upper layer current vectors for (a) October 16, (b) December 16, (c) January 15, (d) January 30, (e) February 14, and (f) March 1 of a climatological year forced by the *Hellerman and Rosenstein* [1983] mean monthly wind stress values. Only a portion of the model domain is depicted. The contour interval is 3 cm.

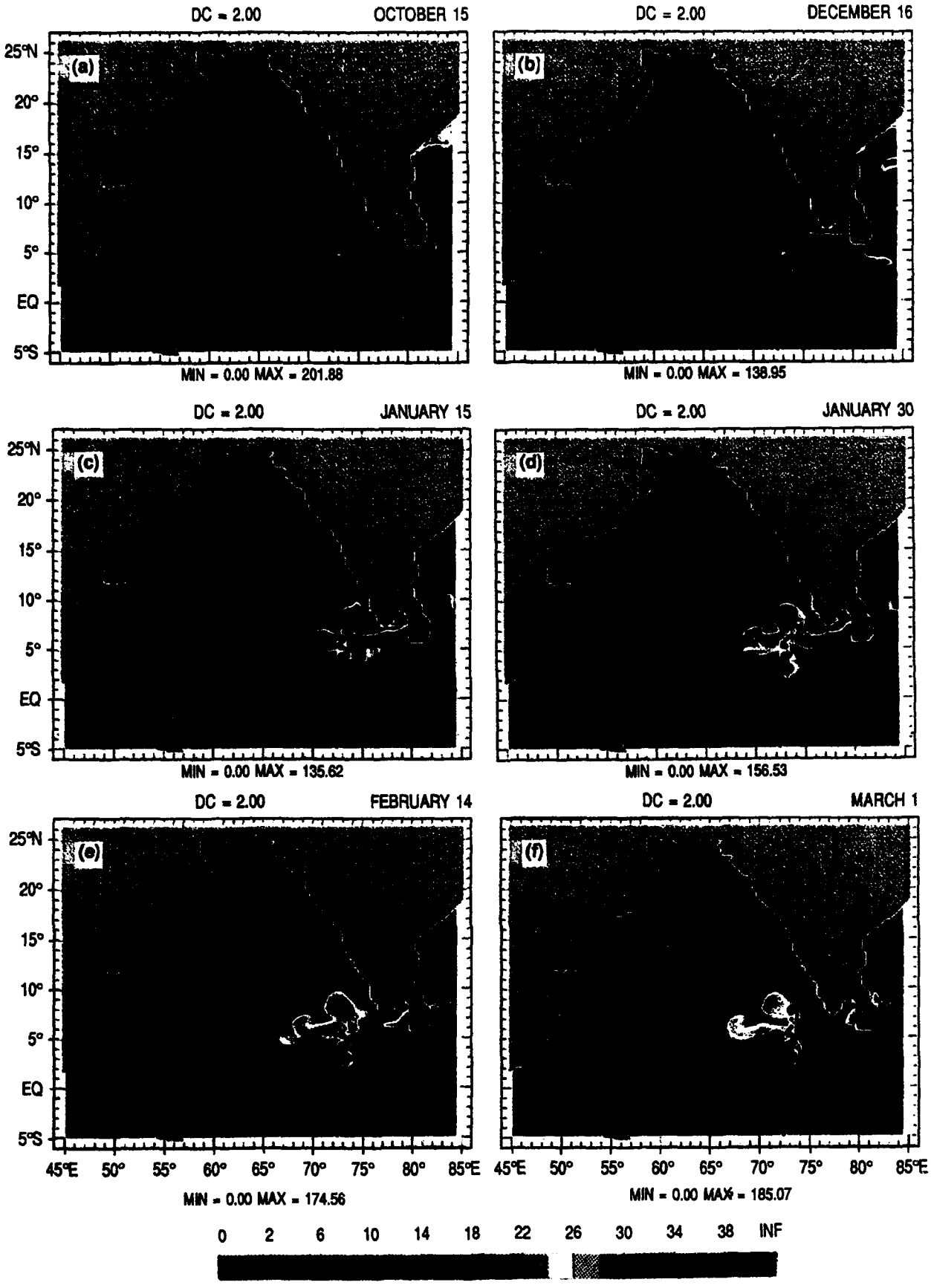

Plate 3. Snapshots of the model tracer whose source region is in the Bay of Bengal (see text) for the same days as in Plate 2.

Summary and Discussion

The LH is a large anticyclonic eddy that consistently appears near the southwestern tip of India during the NE monsoon season. It grows rapidly in situ from late November to late December at about 10°N over the Laccadive Island Chain. In January it can be seen propagating westward where it dies in midbasin. In our study we have found good agreement in eddy size, location, amplitude, and time of appearance with a variety of observational methods (hydrography, satellite altimetry, and numerical model experiments) covering a number of years of observation. Comparing observations from all three methods and for different years, there is some indication that the eddy's position and characteristics vary interannually but not to a large or (yet) well-defined extent. Some of the principal characteristics of the LH are listed in Table 3.

The numerical tracer study and pattern of fresh water extending from the Bay of Bengal [*Wyrtki*, 1971] strongly suggests a connection between the LH and the Bay of Bengal Water via the NEC. Both model and climatological surface currents [*Cutler and Swallow*, 1984] depict a bifurcation of the NEC in January in the near-equatorial region south of India. The northern branch, which is established in December, loops around the south coasts of Sri Lanka and India and appears to be an integral component of the LH genesis. As this water then turns back toward the coast of India, part continues northward along the coast, and part continues to turn in the anticyclonic motion of the high-pressure LH. *Shetye et al.* [1991] examine coastal currents off western India during the NE monsoon. Although only limited evidence of the LH can be seen in their hydrographic surveys, they do find an alongshore pressure gradient (positive equatorward) during December/January, which is consistent with the appearance of the LH. From surface salinity charts of their survey it can be seen that the low-salinity Bay of Bengal Water is confined to the southern part of the west coast, suggesting that the recirculation pattern in the LH tends to block the flow of this fresher water northward. Wyrtki's chart (Figure 2) shows only a moderate extension of low-salinity water (i.e., <34‰) toward the north, some of which may be due to local runoff.

Two previous numerical studies are useful in attempting to determine the generating mechanism(s) of the LH. *Yu et al.* [1991] (hereinafter referred to as YOY) and *McCreary et al.* [1993] (hereinafter referred to as MKM) have both examined the relative importance of remote and local forcing to the circulation in this region. Although not discussed directly by YOY, an anticyclonic feature in the region of the LH appears during the NE monsoon season of their reduced-gravity oceanic model. The study used two wind-forcing patterns: (1) a seasonally varying wind stress confined to within ±5° of the equator and (2) a seasonal wind stress contained entirely within the idealized Bay of Bengal. The first pattern produced a weak anticyclone off the southwest coast of India during February. The feature appeared (our inference) to be generated by wind-forced, downwelling, coastal kelvin waves that leaked energy offshore via westward propagating long Rossby waves. The source of the coastal kelvin waves could be traced back to wind stress in the equatorial wave guide, or possibly to wind stress immediately adjacent to the idealized south coast of India/Sri Lanka. The second pattern of winds (i.e., those confined to the Bay of Bengal) did produce a minor high in the area of the LH, but not a LH-like feature, suggesting that remote forcing from within the Bay of Bengal does not contribute significantly to the generation of the LH.

MKM also studied the effect of remote forcing on Indian Ocean circulation patterns. In a similar fashion to the study of YOY, but with a more realistic basin and wind system, MKM shut off wind forcing in various parts of the basin, and compared the results to a main run solution. In two cases of interest, when winds were shut off separately over the Bay of Bengal and over the Arabian Sea, an anticyclonic structure appeared in each case off the southwestern coast of India during January. These studies would suggest that both local and remote forcing participate in the formation of the LH. In the study of MKM, however, it should be noted that their Bay of Bengal winds included the equatorial waveguide east of India, while the study of YOY did not, indicating that winds between the equator and 10°N are the most important to remote forcing of the LH.

The principal objective of this study has been to point out the existence of the LH, using a variety of observational and modeling means, and to present some of its most salient characteristics. Modeling studies, designed for other purposes, have suggested that both local and remote forcing are influential in the formation of the LH. This is an aspect which needs to be addressed by future modeling and observational studies focused on this phenomenon.

Acknowledgments. This work is a contribution to the Naval Research Laboratory (NRL) 6.1 Biology-Ocean Dynamics Coupling Project under program element 61153N sponsored by the Office of Naval Research. One of us (J.B.) is grateful to the Naval Oceanographic Office for support, and one of us (D.J.) is grateful to the Minerals Management Service's Gulf of Mexico Basin Scale Modeling Project for support. Appreciation is also extended to J. Pringle for incorporating the tracer formulation into the model and to W. Youtsey for his programming and analysis assistance. R. Cheney (NOAA) very kindly provided much of the altimetry data. V. Ladner gave us much appreciated editorial support, and J. Lewandoski gave technical support with the altimetry data. The numerical simulation was performed on the Primary Oceanographic Prediction System CRAY Y-MP 8/8128 at the Naval Oceanographic Office. NRL contribution number NRL/JA/7332-93-0010.

References

Arnault, S., and C. Perigaud, Altimetry and Models in the tropical oceans: A review, *Oceanol. Acta*, *15*, 411–430, 1992.

Bauer, S., G. L. Hitchcock, and D. B. Olson, Influence of monsoonally-forced Ekman dynamics upon surface layer depth and plankton biomass distribution in the Arabian Sea, *Deep Sea Res.*, *38*, 531–553, 1991.

Bruce, J. G., Comparison of near surface dynamic topography during the two monsoons in the western Indian Ocean, *Deep Sea Res.*, *15*, 665–667, 1968.

Bruce, J. G., Eddies off the Somali coast during the southwest monsoon, *J. Geophys. Res.*, *84*, 7742–7748, 1979.

Bruce, J. G., Variations in the thermal structure and wind field occurring in the western Indian Ocean during the monsoons, *Tech. Rep. TR 272*, Nav. Oceanogr. Off., Stennis Space Cent., Miss., 1981.

Bruce, J. G., and W. H. Beatty, Some observations of the coalescing of the Somali eddies and a description of the Socotra eddy, *Oceanol. Acta*, *78*, 207–219, 1985.

Cheney, R. E., and L. Miller, GEOSAT altimeter Indian Ocean sea level analysis, in *Climate Diagnostics Bulletin, Dec. 1988 to April 1989*, Climate Analysis Center, National Oceanic and Atmospheric Administration, Washington, D. C., 1988–1989.

Cheney, R. E., L. Miller, R. W. Agreen, N. S. Doyle, and B.

Douglas, Monitoring tropical sea level in near-real time with GEOSAT altimetry, *Johns Hopkins APL Tech. Digest, 10*, No. 4, *1989*.

Cutler, A. N., and J. C. Swallow, Surface currents of the Indian Ocean (to 25°S, 100°E), *I.O.S. Tech. Rep.*, 187 pp., 1984.

Findlater, J., Observational aspects of the low-level cross-equatorial jet stream of the western Indian Ocean, *Pure Appl. Geophys., 115*, 1251–1262, 1977.

Fu, L.-L., and D. B. Chelton, Observing large-scale temporal variability of ocean currents by satellite altimetry: With application to the Antarctic Circumpolar Current, *J. Geophys. Res., 90*, 4721–4739, 1985.

Hastenrath, S., and P. J. Lamb, *Climatic Atlas of the Indian Ocean, Part 1, Surface Circulation and Climate*, 104 pp., University of Wisconsin Press, Madison, 1979.

Hellerman, S., and M. Rosenstein, Normal monthly wind stress over the world ocean with error estimates, *J. Phys. Oceanogr., 13*, 1093–1104, 1983.

Hurlburt, H. E., and J. D. Thompson, A numerical study of Loop Current intrusions and eddy shedding, *J. Phys. Oceanogr., 10*, 1611–1651, 1980.

Johnson, D. R., J. D. Thompson, and J. D. Hawkins, Circulation in the Gulf of Mexico from Geosat altimetry during 1985–1986, *J. Geophys. Res., 97*, 2201–2214, 1992.

Kindle, J. C., Topographic effects on the seasonal circulation of the Indian Ocean, *J. Geophys. Res.*, 96(C9), 16,827–16,837, 1991.

Kindle, J. C., and J. D. Thompson, The 26- and 50-day oscillations in the western Indian Ocean: Model results, *J. Geophys. Res., 94*(C4), 4721–4736, 1989.

Levitus, S., Climatological atlas of the world ocean, *Prof. Pap., 13*, 173 pp., Natl. Oceanic and Atmos. Admin., Rockville, Md., 1982.

Luther, M. E., and J. J. O'Brien, A model of the seasonal circulation in the Arabian Sea forced by observed winds, *Prog. Oceanogr., 14*, 353–385, 1985.

McCreary, J. P., P. K. Kundu, and R. L. Molinari, A numerical investigation of dynamics, thermodynamics and mixed-layer processes in the Indian Ocean, *Prog. Oceanogr., 31*, 181–244, 1993.

Molinari, R. L., D. Olson, and G. Reverdin, Surface current distributions in the tropical Indian Ocean derived from compilations of surface buoy trajectories, *J. Geophys. Res., 95*, 7217–7238, *1990*.

Naval Air Weather Service, *U.S. Navy Marine Climatic Atlas of the World*, vol. III, *Indian Ocean*, NAVAIR 50-1C-530, Washington, D. C., 1976.

O'Brien, J. J., and H. E. Hurlburt, Equatorial jet in the Indian Ocean: Theory, *Science, 184*, 1075–1077, 1974.

Perigaud, C., and P. Delecluse, Annual sea level variations in the southern tropical Indian Ocean from GEOSAT and shallow-water simulations, *J. Geophys. Res., 97*, 20,169–20,178, 1992.

Perigaud, C., and J. F. Minster, Variability of the Somali Current as observed from SEASAT altimetry, *J. Phys. Oceangr., 102*, 25–39, 1988.

Shetye, S. R., A. D. Gouveia, S. S. C. Shenoi, G. S. Michael, D. Sundar, A. M. Almeida, and K. Santanam, The coastal current off western India during the northeast monsoon, *Deep Sea Res., 38*, 1517–1529, 1991.

Wallcraft, A. J., The navy layered ocean model users' guide, *Rep. 235*, 21 pp., Nav. Res. Lab., Stennis Space Cent., Miss., 1991.

Wyrtki, K., *Oceanographic atlas of the International Indian Ocean Expedition*, 531 pp., U.S. Government Printing Office, Washington, D. C., 1971.

Wyrtki, K., An equatorial jet in the Indian Ocean, *Science, 181*, 262–264, 1973.

Yu, L., J. J. O'Brien, and J. Yang, On the remote forcing of the circulation in the Bay of Bengal, *J. Geophys. Res., 96*, 20,449–20,454, 1991.

J. G. Bruce, Naval Oceanographic Office, Code N341, Stennis Space Center, MS 39522-5001.

D. R. Johnson and J. C. Kindle, Naval Research Laboratory, Code 7332, Stennis Space Center, MS 39529-5004.

(Received May 18, 1993; revised August 23, 1993; accepted September 10, 1993.)